

Substrate Flow in Catalases Deduced from the Crystal Structures of Active Site Variants of HP11 from *Escherichia coli*

William Melik-Adamyán,¹ Jerónimo Bravo,² Xavier Carpena,² Jack Switala,³ Maria J. Maté,² Ignacio Fita,² and Peter C. Loewen^{3*}

¹*Institute of Crystallography, Russian Academy of Sciences, Moscow, Russia*

²*Instituto Biología Molecular Barcelona (C.S.I.C.), Barcelona, Spain*

³*Department of Microbiology, University of Manitoba, Winnipeg, Manitoba, Canada*

ABSTRACT The active site of heme catalases is buried deep inside a structurally highly conserved homotetramer. Channels leading to the active site have been identified as potential routes for substrate flow and product release, although evidence in support of this model is limited. To investigate further the role of protein structure and molecular channels in catalysis, the crystal structures of four active site variants of catalase HP11 from *Escherichia coli* (His128Ala, His128Asn, Asn201Ala, and Asn201His) have been determined at ~2.0-Å resolution. The solvent organization shows major rearrangements with respect to native HP11, not only in the vicinity of the replaced residues but also in the main molecular channel leading to the heme distal pocket. In the two inactive His128 variants, continuous chains of hydrogen bonded water molecules extend from the molecular surface to the heme distal pocket filling the main channel. The differences in continuity of solvent molecules between the native and variant structures illustrate how sensitive the solvent matrix is to subtle changes in structure. It is hypothesized that the slightly larger H₂O₂ passing through the channel of the native enzyme will promote the formation of a continuous chain of solvent and peroxide. The structure of the His128Asn variant complexed with hydrogen peroxide has also been determined at 2.3-Å resolution, revealing the existence of hydrogen peroxide binding sites both in the heme distal pocket and in the main channel. Unexpectedly, the largest changes in protein structure resulting from peroxide binding are clustered on the heme proximal side and mainly involve residues in only two subunits, leading to a departure from the 222-point group symmetry of the native enzyme. An active role for channels in the selective flow of substrates through the catalase molecule is proposed as an integral feature of the catalytic mechanism. The Asn201His variant of HP11 was found to contain unoxidized heme b in combination with the proximal side His–Tyr bond suggesting that the mechanistic pathways of the two reactions can be uncoupled. *Proteins* 2001;44:270–281.

© 2001 Wiley-Liss, Inc.

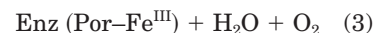
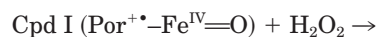
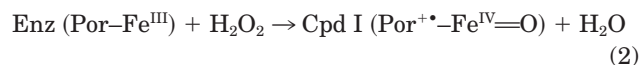
Key words: crystal structure; catalase; catalysis; protein channels

INTRODUCTION

Catalase (hydrogen peroxide:hydrogen peroxide oxidoreductase, EC 1.11.1.6), present in most aerobic organisms, is a protective enzyme that removes hydrogen peroxide before it can decompose into highly reactive hydroxyl radicals. The characteristic catalase activity—the catalytic reaction—uses hydrogen peroxide as both an electron donor and an electron acceptor, as summarized in the overall reaction 1:



This reaction takes place in two distinct stages: in the first stage (reaction 2) the resting state enzyme is oxidized by hydrogen peroxide to an intermediate, compound I, which in the second stage (reaction 3) is reduced back to the resting state by a second hydrogen peroxide:



The structures of heme catalase isolated from seven different sources have now been solved, including those from bovine liver,^{1,2} human erythrocytes,^{3,4} *Penicillium vitale*,^{5,6} *Saccharomyces cerevisiae*,⁷ *Proteus mirabilis*,⁸ *Micrococcus lysodeikticus*,⁹ and *Escherichia coli*,^{10,11} revealing a

Grant sponsor: DGICYT (Spain); Grant number: BIO099-0865; Grant sponsor: European Union; Grant number: CHGE-CT93-0040; Grant sponsor: Natural Sciences and Engineering Research Council of Canada (NSERC); Grant number: RGP9600; Grant sponsor: NATO; Grant number: SA-5-2-05; Grant sponsor: MEC (Spain); Grant number: SAP 1998-0087.

William Melik-Adamyán and Jerónimo Bravo contributed equally to this work.

Jerónimo Bravo is currently at the MRC Laboratory of Molecular Biology, Hills Road, Cambridge CB2 2QH, UK.

*Correspondence to: Peter Loewen, Department of Microbiology, University of Manitoba, Winnipeg, MB R3T 2N2 Canada. E-mail: peter_loewen@umanitoba.ca

Received 8 December 2000; Accepted 22 March 2001

common, highly conserved, core structure in all enzymes. The heme active center in catalase HPII from *E. coli* shares with all other catalases the structural features that are important for catalysis, in particular the presence and relative orientation of a histidine (His128) and an asparagine (Asn201) on the distal side of the heme and a tyrosine (Tyr415) on the proximal side (Fig. 1A). However, HPII is unique among catalases in having two posttranslational modifications in the vicinity of the active center, which are self-catalyzed after the adoption of the final quaternary structure. One of the modifications, also found in some other large subunit catalases,¹² is an oxidized heme group, in the form of a *cis*-spirolactone, termed heme d. The second modification, so far unique to HPII, is a covalent bond between the N^δ of His392 and the C^β of Tyr415, the proximal side fifth ligand of the heme.¹³ Both modifications seem to require some degree of catalytic activity, and it has been proposed, based on the properties of a number of HPII variants¹¹, that compound I acts as an initiator of these modifications with a possible mechanistic relationship between the two reactions.

A number of catalase HPII variants have been constructed that incorporate changes into the catalytic residues, His128 and Asn201, on the distal side of the heme. Replacement of His128 with any one of a number of residues results in variants with no detectable activity or in variants that are defective in folding, such that no protein accumulates.¹⁴ Replacement of Asn201 with aspartate, glutamine, alanine, or histidine causes a reduction in specific activity to less than 10% of wild-type levels, but in no case does activity become nondetectable.¹⁴ On the basis of these data, it was concluded that His128 is essential for the enzymatic activity, while Asn201 facilitates catalysis, but is not essential.

Despite all the structural and biochemical information about catalases that has accumulated over 100 years, a number of basic questions remain unanswered, among them: (1) how efficient substrate flow toward the deeply buried active centers is achieved; and (2) the basis of the specificity for hydrogen peroxide. To address these issues, a structural determination of variants of the active site residues His128 and Asn201 was undertaken. The complete absence of activity in the His128 variants also allowed the isolation and structural analysis of complexes between the protein and hydrogen peroxide. Data obtained provide significant insights into the roles of molecular channels and protein structure in the mechanism of catalysis.

METHODS

The four HPII variant proteins analyzed in this work were purified from the catalase deficient *E. coli* UM255 as previously described.¹⁴ Crystals were obtained at room temperature by the vapor diffusion hanging drop method at a protein concentration of ~15 mg/ml over a reservoir containing 15–17% PEG 3350, 1.6–1.5 M LiCl and 0.1 M Tris-HCl, pH 9 as previously described for native HPII.¹¹ Crystals were monoclinic space group P2₁ with one tetrameric molecule in the crystal asymmetric unit. Diffraction

data for the His128Ala, His128Asn, and Asn201Ala variants were obtained from crystals transferred to a solution containing 30% PEG 3350 and flash-cooled with a nitrogen cryo-stream, yielding the following unit cell parameters: $a = 93.0 \text{ \AA}$, $b = 132.3 \text{ \AA}$, $c = 121.2 \text{ \AA}$ and $\beta = 109.3^\circ$. Data collection for the isomorphous crystals of the Asn201His variant was carried out at room temperature, yielding the following unit cell parameters: $a = 95.2 \text{ \AA}$, $b = 134.7 \text{ \AA}$, $c = 124.4 \text{ \AA}$ and $\beta = 109.4^\circ$. The four diffraction data sets were processed using the program DENZO and scaled with program SCALEPACK.¹⁵ In this study, 5% of the measured reflections in every data set was reserved for R_{free} monitoring during automatic refinement (Table I).

Refinement of the four variants was carried out with the program XPLOR using standard protocols.¹⁶ For each variant, the starting model was the HPII structure refined to 1.9 \AA .¹³ Coordinates were readjusted to the corresponding unit cells using the option balloon of XPLOR, and the position of the molecule was then refined with some cycles of rigid body refinement. Altered residues and neighbor solvent molecules were always omitted in the starting models. Refinements were completed using the program REFMAC¹⁷ with solvent molecules modeled either automatically using ARPP¹⁸ or manually with the graphic program O.¹⁹ Solvent molecules were only introduced when they corresponded to the strongest peaks in the difference Fourier maps that could make at least one hydrogen bond with atoms already in the model. In the final rounds of refinement, the four subunits were treated independently with the bulk solvent correction applied and the whole resolution range available used for each variant. To ensure the consistency of the differences found in the HPII variant structures, the native HPII was also re-refined using the same procedures (Table I). In the five structures obtained, the analysis of solvent accessibility and molecular cavities was carried out with program VOIDOO²⁰ using a reduced atomic radius for polar atoms in accounting for possible hydrogen bonds.²¹

Structure factors and coordinates are accessible from PDB with identification codes 1GGE, 1GG9, 1GGF, 1GGH, 1GGJ, and 1GGK, respectively, for native HPII, His128Asn, His128Asn-H₂O₂, His128Ala, Asn201Ala, and Asn201His variants.

RESULTS

Quality of the Variant HPII Structures

Like the structure of native HPII,^{12,13} the crystal asymmetric units of the four HPII variants analyzed in this study (His128Ala, His128Asn, Asn201Ala, and Asn201His) contain homotetramers with 3,012 amino acids. The N-terminal 26 residues of all subunits in the four variants remain disordered, as in the native enzyme, and are not included in the refined structures. Crystallographic agreement R and R_{free} factors and relevant refinement statistics for the structures of the four variants are similar to the ones obtained for the native enzyme, particularly for the His128Asn and the Asn201Ala variants determined at about the same resolution as native HPII (Table I). The quality and resolution of the diffraction data are slightly

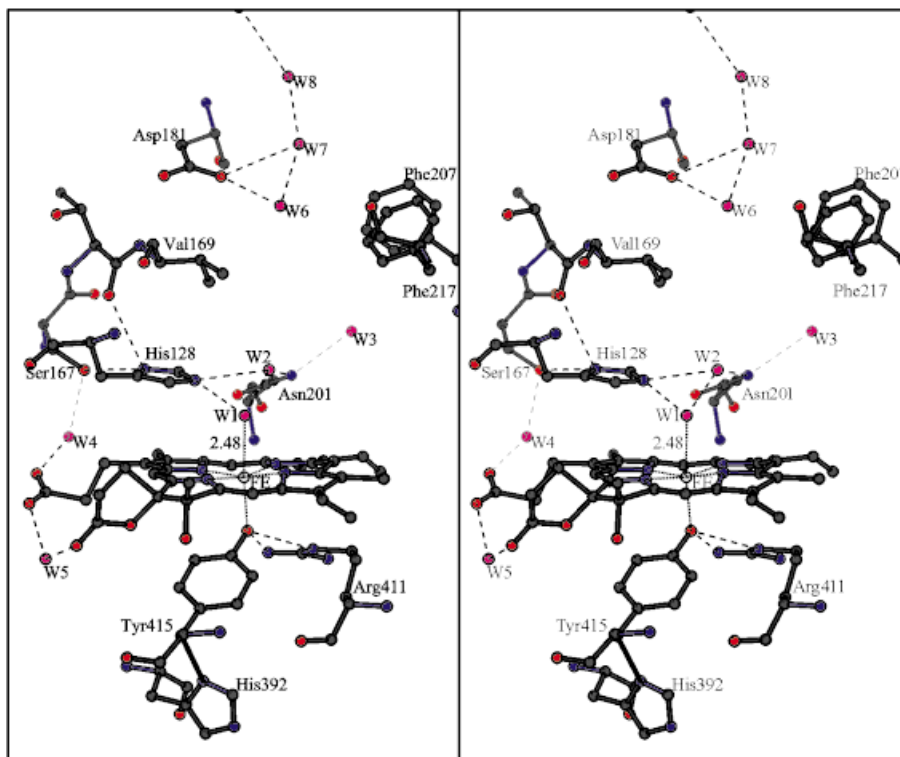
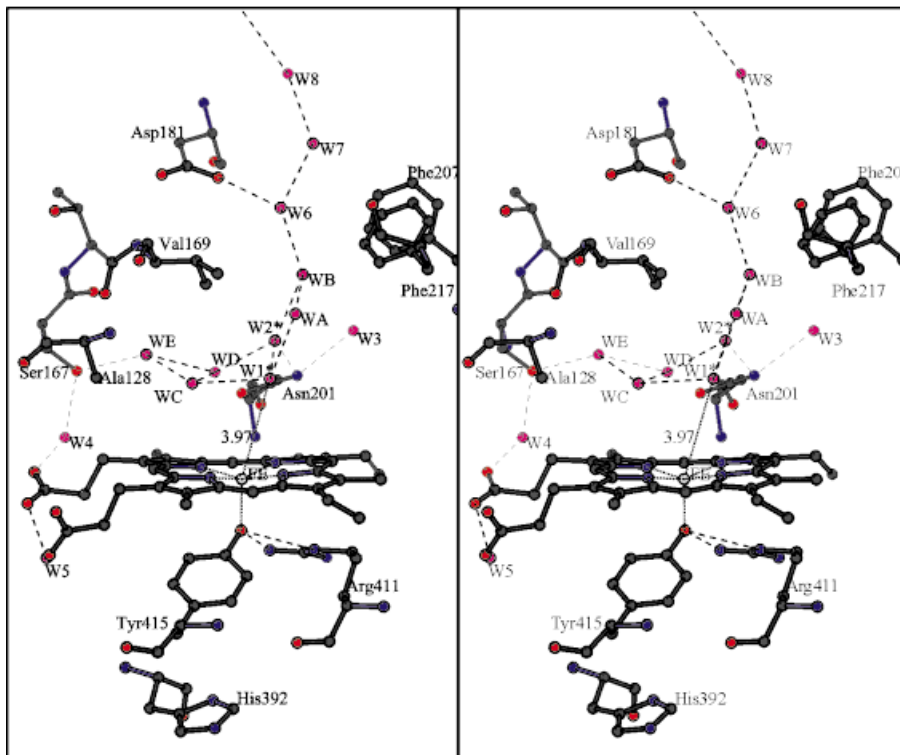
A - HP11**B - H128A**

Figure 1.

C - N201H

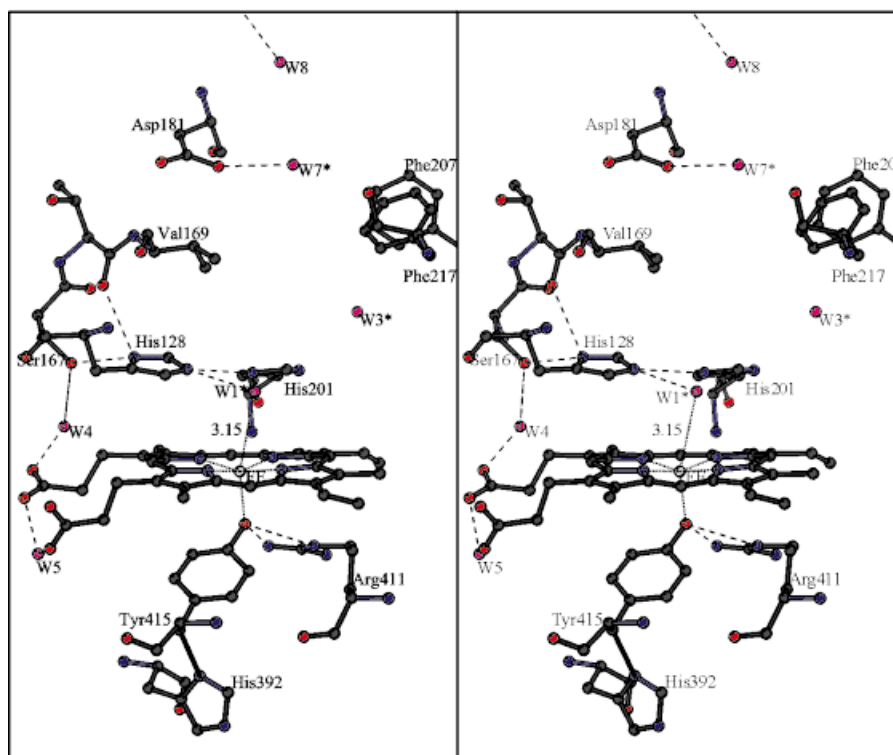


Fig. 1. Stereo views of the heme environment. **A:** Native HP11. **B:** His128Ala variant. **C:** Asn201His variant. For clarity, only the catalytically important residues His128, Ser167, and Asn201 on the heme distal side and His392, Arg411, and Tyr415 on the heme proximal side are explicitly shown. Also displayed are the conserved residues lining the channel, Val169, Asp181, Phe207, and Phe217. The ring of hydrophobic residues that include Val169 define the narrowest point in the major channel. Heme d is evident only in native HP11 (**A**), and the covalent bond between the side-chains of His392 and Tyr415 is evident in native HP11 (**A**) and the Asn201His variant (**C**). Changes in solvent organization are evident among the three structures. Water molecules in the native enzyme, and their equivalent in the variants, are labeled numerically, W1–W8. Water molecules in the variant structures with no correspondence in native HP11 are labeled alphabetically, WA–WE. [Color figure can be viewed in the online issue, which is available at www.interscience.wiley.com.]

lower for the Asn201His variant structure, probably a result of data collection at room temperature. The quality and resolution of the His128Asn crystals soaked in H_2O_2 permitted accurate determination of differences in the protein structure and in the solvent organization caused by the soaking.

Structural Differences of the HP11 Variants With Respect to the Native Enzyme

The absence of the imidazole group of His128, the distal side essential histidine of HP11, precludes the formation of compound I and results in all variants of His128 lacking catalytic activity.¹⁴ The His128Ala variant is no exception, with no activity over background levels being detectable even at very high protein concentrations (Table II). The structure of this variant reveals the expected methyl group of Ala128 above ring IV of the heme b (note the propionate side-chain in Fig. 1B, as compared with the spirolactone ring in the heme d of the native enzyme in Fig. 1A) in place of the imidazole ring of histidine in native HP11. Despite the increased accessibility to the iron atom in the variant resulting from the small size of the alanine residue, the

closest solvent molecule is ~ 4.0 Å from the heme iron, even farther away than in the native enzyme, indicative of the very weak binding of water in the sixth coordination position. The presence of heme b, rather than heme d, and the absence of the His392–Tyr415 covalent linkage are consistent with the total absence of catalytic activity in this variant.¹⁴ The propionate group from ring III of the unmodified heme b is hydrogen bonded with the nearby Gln419 residue, which also interacts with an adjacent water molecule. An identical rearrangement had already been found in other HP11 variants that contain heme b.¹⁰ The imidazole group of His392, not covalently linked to Tyr415, is rotated with respect to the orientation seen in the native enzyme (Fig. 1A,B). Other than the changes just described and the extensively altered solvent organization described below, the His128Ala variant protein is essentially identical in structure to native HP11, particularly in the heme distal side pocket.

The His128Asn variant also lacks all detectable catalytic activity, attributable to the absence of the essential imidazole ring (Table II). Aside from the obvious presence of the asparagine side-chain interacting with the main-

TABLE I. Data Collection and Structural Refinement Statistics

	Protein					
	Native	H128A	H128N	N201H*	N201A	HP-H128N
A. Data collection statistics						
Resolution range (Å)	18/1.89	15/2.15	15/1.89	13/2.26	19/1.92	19.8/2.28
Unique reflections	214389	143588	196776	120733	193708	125885
Completeness (%)	97.7	95.9	89.5	88.2	91.7	98.5
$\langle F \rangle / \langle \sigma(F) \rangle$	11.17	10.21	10.81	14.54	6.45	10.9
R_{sym} (%)	8.9	10.5	8.7	8.9	13.9	10.7
<i>In the last shell</i>						
Resolution range (Å)	1.94/1.89	2.21/2.15	1.94/1.89	2.32/2.36	1.97/1.92	2.34/2.28
Unique reflections	16094	11135	16215	10095	15468	9488
Completeness (%)	88.4	93.3	80.2	68.4	89.5	95.9
$\langle F \rangle / \langle \sigma(F) \rangle$	5.00	5.25	4.32	6.67	3.13	4.11
R_{sym} (%)	26.9	26.4	27.5	35.5	49.0	36.5
B. Refinement statistics						
Working set	203615	136412	186868	114621	184003	119537
Free reflections	10744	7176	9907	6111	9705	6348
R_{cryst} (%)	16.6	16.1	15.9	14.3	19.4	18.5
R_{free} (%)	20.2	20.6	18.8	20.8	23.5	25.4
<i>In the last shell</i>						
R_{cryst} (%)	18.9	17.1	17.9	18.3	24.9	19.8
R_{free} (%)	23.2	22.8	21.9	27.1	28.8	29.6
<i>No. of nonhydrogen atoms</i>						
Protein	22984	22964	22984	22992	22984	22964
Heme	176	172	172	172	176	172
Water	3208	2828	3439	1723	2802	2036
Hydrogen peroxide	—	—	—	—	—	12
<i>RMSD from ideality</i>						
Bond distances (Å)	0.008	0.008	0.007	0.010	0.008	0.009
Angle distances (Å)	0.025	0.027	0.023	0.031	0.025	0.031
Planarity (Å)	0.019	0.019	0.018	0.020	0.018	0.020
Chiral volume (Å ³)	0.114	0.110	0.103	0.121	0.103	0.117
<i>Averaged B factors (Å²)</i>						
Main-chain	10.6	11.0	10.4	19.2	8.6	24.2
Side-chain	11.9	12.6	13.3	20.8	10.7	24.3
Water	18.6	17.5	20.6	24.1	17.2	21.0

RMSD, root-mean-square deviation.

TABLE II. Catalytic Activity and Posttranslational Modifications

Variant	Heme	Tyr415–His392	Activity units/mg
Native	d	y	15,200
His128Ala	b	n	<0.1
His128Asn	b	n	<0.1
His128Asn–H ₂ O ₂	b	n	—
Asn201Ala	d	y	1,300
Asn201His	b	y	100

chain oxygen of residue 168, the protein structure of the His128Asn variant is very similar to that of the His128Ala variant including the absence of the His392–Tyr415 covalent bond and the presence of heme b, with all the

concomitant readjustments described above for the His128Ala structure.

The Asn201Ala variant exhibits about 10% of native HP11 catalytic activity (Table II), indicating that residue Asn201 has a major, but not completely essential, role in catalysis. On the distal side of the heme, the most obvious change in the protein structure of the variant is the expected absence of the amide group of the asparagine side-chain. The heme is oxidized to heme d, consistent with the previously reported biochemical characterization of heme d in this variant,¹⁴ and the His392–Tyr415 bond is also evident, making the structure in this region very similar to that of native HP11 (Fig. 1A). The fact that both heme oxidation and His–Tyr bond formation occur despite the reduced catalytic activity, confirms that even a slow generation of compound I is sufficient to promote both reactions.

The Asn201His variant exhibits less than 1% of native HP11 catalytic activity (Table II). This reduction can be explained by a combination of the absence of the catalytic asparagine and by the reduction of the distal pocket volume due to the presence of the bulkier imidazole group in the variant. The N^ε atoms of the two imidazole groups found in the heme distal side of the Asn201His variant (His128 and His201) are hydrogen bonded to each other with N^ε from His128 acting as the hydrogen acceptor (Fig. 1C). As a result, atom N^δ from His201 is deprotonated explaining the absence of a hydrogen bond with water molecule W3*. In native HP11, the corresponding water molecule (W3 in Fig. 1A) stabilizes the appropriate orientation of the Asn201 side-chain for it to act as a hydrogen acceptor. The Asn201His variant was characterized biochemically as containing only heme b,¹⁴ as confirmed in the current structural analysis. Surprisingly, the structure shows clear evidence for the presence of the His–Tyr bond (Fig. 1C), providing the first evidence that the two self-catalyzed posttranslational modifications can be uncoupled in HP11.

Solvent Reorganization in the HP11 Variants With Respect to the Native Enzyme

In addition to the structural differences compared with native HP11 described above, the four active site variants reveal striking reorganizations of the solvent both near the replaced residues and in the main channel leading to the heme distal pocket (Figs. 1–3). Three of the variants, His128Asn, His128Ala, and Asn201Ala, all have a larger number of water molecules in these regions than the native enzyme, while the Asn201His variant, with a bulkier residue introduced, contains fewer.

More significant than changes in the number of waters are changes in the distribution of the waters in the variants as compared with native HP11. In most catalases, including HP11, there are two water molecules (indicated as W1 and W2 in Fig. 1A) hydrogen bonded to each other, that bridge the essential histidine and asparagine residues in the heme distal side pocket. W1, which acts as a hydrogen donor in its interaction with atom N^ε from His128, is the solvent molecule closest to the heme iron atom (at a distance of ~2.5 Å) and in native HP11 presents either a low occupancy or a high mobility.¹³ The second water, W2, with full occupancy or low mobility, is bound to N^δ from Asn201. Three additional solvent molecules (W3, W4, and W5 in Fig. 1A), situated in close proximity to the heme, are also well conserved among catalases. Proceeding up the main channel away from the distal side heme pocket, the first well defined solvent molecule in the main channel (W6 in Fig. 1A) is approximately 7 Å from W2, and is hydrogen bonded to an aspartate residue (Asp181 in HP11) conserved in all catalase sequences. The absence of any other well defined solvent molecules in the lower part of the main channel leaves a large gap between W2 and W6, which is apparently empty (Fig. 1A). From W6, a chain of hydrogen bonded solvent molecules extends up the channel to the molecular surface.

In the His128Ala variant (Figs. 1B, 2), replacement of the imidazole ring with the much smaller methyl side-chain of alanine increases the size of the active site cavity, but also removes a side-chain capable of forming hydrogen bonds. It is therefore somewhat surprising to find that the number of water molecules in this region increases substantially to seven from two in native HP11. The five water molecules in the variant, without equivalent in the native structure, are indicated as WA to WE in Figure 1B. The appearance of waters WA and WB in the narrowest and most hydrophobic part of the channel provides continuity to the chain of solvent molecules extending from the heme distal pocket to the molecular surface. The displacement of W2*, with respect to the position of the corresponding water W2 in the native enzyme, reduces the distance between W2* and W6, allowing water WB to interact with the two.

The pattern of water molecules in the His128Asn variant is very similar to that just described for the His128Ala variant, with the exception that water WE is missing, displaced by the larger asparagine side-chain at position 128 (Fig. 3A). The presence of two asparagines (Asn128 and Asn201) stabilizes the water molecules, filling the distal side pocket and becoming part of a continuous chain of waters extending to the molecular surface (Fig. 3A). Waters WA and WB in the His128Asn variant are in almost identical locations to the corresponding waters found in the His128Ala variant. Again the reduced distance between W2* and W6 is bridged by the single water WB.

The replacement of asparagine by histidine in the Asn201His variant creates yet another striking organization of solvent molecules (Fig. 1C). In the heme distal side pocket, there is only one defined water molecule, at about the same position as W1 in the native enzyme, likely a result of the reduction in pocket volume arising from the larger size of the imidazole side-chain. Even more surprising is the altered solvent structure around the Asp181 residue, remote from His201, which clearly demonstrates the subtle interdependencies among the solvent binding sites.

The Asn201Ala variant has a poorly defined solvent structure in the vicinity of the heme. There are several water molecules with large mobility or partial occupancies, probably due to the increased cavity size and absence of a side-chain capable of forming hydrogen bonds. Significantly, W3* in this variant is in an almost identical position to W3 in the native enzyme, despite the lack of interactions with the replaced residue Ala201. The stability of W3 provides further support for its critical role in defining the orientation of the side-chain of Asn201 in the native enzyme (see above). Despite the increased cavity volume, the absence of a stable W2* seems to prevent a water from occupying position WB. These data confirm that minor changes in the heme distal side pocket can alternatively stabilize or destroy the continuity of solvent molecules in the hydrophobic part of the channel.

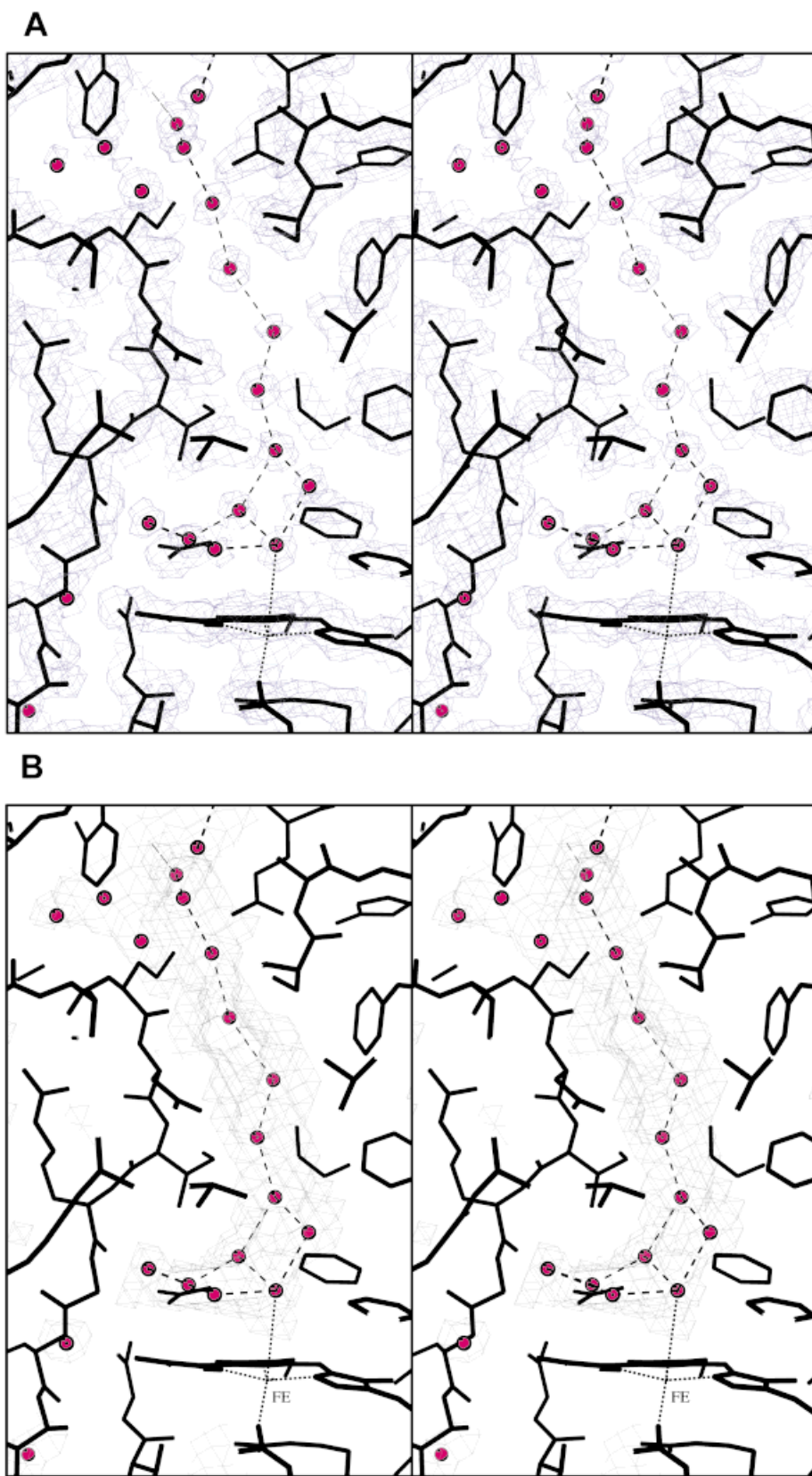


Fig. 2. Stereo views showing the opening of the major channel into the heme distal side pocket in the His128Ala variant structure. **A:** Averaged omit ($F_o - F_c$) electron-density map shown with a chicken wire representation. Density corresponding to the chain of omitted water molecules is clearly defined filling the heme distal side pocket and the major channel. **B:** The accessible surface, calculated with the program VOIDOO, emphasizes the continuity of the channel and of the chain of solvent molecules found inside. Red spheres, water molecules; dashed lines, hydrogen bonds among water molecules in the channel; dotted lines, iron coordination.

TABLE III. Temperature Factors (\AA^2) of the Hydrogen Peroxide Molecules

H_2O_2	Atom	Subunit			
		1	2	3	4
H1	O1	29.0	25.5	35.7	22.0
	O2	29.1	28.6	34.8	21.7
H2	O1	16.1	17.9	20.5	18.3
	O2	13.8	19.0	21.4	18.5
H3	O1	22.6	31.3	18.8	23.4
	O2	25.1	32.3	18.7	21.7

His128Asn HP11 Variant in Complex With H_2O_2

It has not yet been possible to trap hydrogen peroxide inside the structure of active catalases because of the rapid reaction and evolution of O_2 causing serious crystal damage upon soaking in hydrogen peroxide solutions. However, using inactive catalase variants could circumvent this problem. Diffraction data from flash cooled crystals of the inactive His128Asn variant, previously soaked for a few seconds in a 2M hydrogen peroxide solution, were obtained at 2.3- \AA resolution. Preliminary analysis of these crystals, using ($F_o^{\text{complexed}} - F_o^{\text{uncomplexed}}$) difference Fourier maps, indicated the presence of several significant structural changes with respect to the structure of the uncomplexed variant (Figs. 3, 4). Therefore, the structure of the complex was refined, following the same protocols as those described above, and using as a starting model the uncomplexed His128Asn variant structure with all the solvent molecules in the distal pocket and in the main channel removed (Table I). A diversity of ($2F_o - F_c$) and ($F_o - F_c$) maps, both unaveraged or fourfold averaged using noncrystallographic symmetry, were obtained. To compute these maps, the solvent molecules to be analyzed were either omitted or included as water or hydrogen peroxide. All these data provided a consistent support for the presence of three hydrogen peroxide molecules in virtually the same locations in all four crystallographically independent subunits (Table III). Two hydrogen peroxide molecules, H1 and H2, are located immediately above the heme interacting with Asn128 and Asn201, and the third peroxide, H3, is located in the main channel interacting with Ser234 and Glu539 (Fig. 3B). The B values of these 12 peroxide molecules are all small in comparison to the mean solvent B factor (Table III), and they provide a clean explanation for the electron density observed both in the heme distal pocket and further up the main channel. From the location of H3, there is a direct connection between the main channels of the two subunits related by the molecular *R*-axis.²²

Unexpectedly, the greatest structural changes in the protein were found remote from these three peroxide molecules on the heme proximal side, clustered around the central cavity in the tetramer (Fig. 4). These changes involve, in particular, residues Arg111, Phe413, Thr416, and Asp417, in the vicinity of Tyr415, the iron proximal ligand. Even more unexpected, was the observation that

the changes occur in only two subunits (related by the *Q*-axis) causing a deviation from the tetrameric symmetry of the native enzyme; in effect; the complex becomes a dimer of structurally nonidentical dimers. Residues Ile129, Met448, Cys438, and Pro439, in the vicinity of the central cavity, also change position, but without affecting symmetry. Solvent molecules in the vicinity of all the displaced residues experience important rearrangements, and a fourth hydrogen peroxide molecule might be situated close to Ile129, although it is not included in the present model. The presence of the fourth peroxide suggests a possible path leading from the proximal side of the heme groups to the center of the tetramer, a path required by the proposed mechanism for heme oxidation and His-Tyr bond formation.^{11,21}

H1, the H_2O_2 situated closest to the heme, interacts with O^δ from Asn128 and with H2, the second H_2O_2 , and is situated between the positions corresponding to the pair of water molecules WC*-W1* in the structure of the uncomplexed variant (Fig. 3A). H2, the best-defined H_2O_2 (Table III) interacts with H1, as already indicated, with the N^δ of Asn128, and with both O^δ and N^δ from Asn201. H2 is situated between the positions corresponding to the pair of water molecules WD-W2 in the uncomplexed variant. Distances between H1 or H2 and W6 are too large to be bridged by a single solvent molecule, and no solvent, either hydrogen peroxide or water, is evident in the lower hydrophobic part of the major channel. Therefore, a high solvent occupancy in this portion of the channel seems to require the additional stabilization provided by the hydrogen bonded matrix of a chain of solvent molecules as in the uncomplexed His128Asn variant.

DISCUSSION**Mechanistic Uncoupling of Heme Oxidation from His-Tyr Bond Formation**

Previous work had suggested a close link between heme oxidation and His-Tyr bond formation in HP11, and a concerted mechanism was proposed.¹¹ Therefore, it was a most unexpected observation to find the His-Tyr bond and unoxidized heme b in the Asn201His variant. Alternative mechanisms treating the two modifications as separate reactions had been considered¹¹ and now appears to be the most likely option in view of this result. The starting point for both modifications continues to be the formation of compound I because its absence, as in the His128 variants, prevents both reactions. The Asn201His variant exhibits only a very low level of activity, which presumably means a low level of compound I formation. The fact that this low level of compound I is sufficient to promote the formation of the His-Tyr bond, but not heme oxidation, suggests that the energy barrier for His-Tyr bond formation is lower than for heme oxidation. One implication of this conclusion is that the *cis*-stereospecific heme oxidation should not be observed in the absence of His-Tyr bond formation; to date, this is the case.²¹ Treatment of the Asn201His variant with either ascorbate or glucose-glucose oxidase, both of which generate low levels of hydrogen peroxide, causes a spectral change from a heme b-type spectrum to a

heme d-type spectrum.¹⁴ Despite this evidence for heme d formation, only heme b could be isolated from the variant, never heme d. Therefore, the reaction pathway to heme oxidation can be initiated and can produce a molecular species that is spectrally similar to heme d, but which cannot be fully converted to heme d and reverts to heme b on extraction in acetone-HCl.

Solvent Flow in Catalase

Small ligands of metalloproteins, such as NO, CO, O₂, or H₂, have important functions in signal transduction, respiration, and catalysis. The question of whether ligand access to active centers requires specific channels and docking sites or proceeds by random diffusion through the protein matrix has recently been addressed with the conclusion that there are a limited number of pathways for ligand migration.²³ Similar questions are also relevant to catalase, where the rapid turnover rate requires an efficient mechanism for H₂O₂ to gain access to, and for products to be exhausted from, the deeply buried active sites. In catalase, the existence of alternative channels suggests a possible directional flow model in which one channel is used for substrate intake and a second (or possibly more than one) is used for product exhaust. The major channel, which enters the heme distal side pocket perpendicular to the heme surface, is highly conserved among all catalases and has long been considered the prime candidate for the inlet channel, although supporting evidence is limited. In small subunit enzymes, like BLC, this channel is ~35 Å in length, but in large subunit enzymes, like HP11, the normal entrance is partially occluded by the C-terminal extension and may be 20 Å longer.¹¹ In both types of catalase, the inner part of the major channel narrows into a constricted region lined with hydrophobic residues that opens into the heme distal side pocket (Figs. 1–3). The constricted hydrophobic portion of the channel, spanning ~7 Å, makes access difficult for molecules larger than water and H₂O₂, presumably helps determine the substrate specificity of the enzyme, and prevents access of potential inhibitors. Recently this portion of the channel has been referred to as a “molecular ruler” as part of a hypothesis that the channel’s dimensions are optimized for hydrogen peroxide,³ but not water, explaining the absence of well-defined water in this section of the channel.

The HP11 variants described in this article demonstrate that any perturbation in the active site of HP11 which stabilizes the inclusion of more waters in the cavity can result in solvent occupancy of the hydrophobic portion of the major channel and in the formation of a continuous chain of water, >30 Å in length, extending from the molecular surface to the active site. In fact, only one or two additional hydrogen bonds are sufficient to stabilize solvent (WA or WB) in the hydrophobic section of the channel. Consequently, the energy barrier to solvent residency in the hydrophobic portion of the major channel is, at most, a few kilojoules per mole (kJ/mol). The larger size of hydrogen peroxide and its greater hydrophilic character compared with water might eliminate this barrier in native

catalases, permitting the formation of a hydrogen-bonded chain extending through the hydrophobic segment of the channel. The stereo-specific requirements underlying the formation of a continuous chain of solvent molecules can help explain the substrate specificity of the enzyme, as well as the apparent fragility of the structural feature.

The unidirectional movement of a chain of substrate molecules, which would facilitate the selective access of H₂O₂ molecules into the active site as the catalytic reaction progresses, requires a separate channel for the exhaust of reaction products. The existence of separate inlet and exhaust channels leading to and from the active site allows a “flow” of molecules through the catalase with H₂O₂ entering by one channel and H₂O and O₂ exiting by different ones. The drive for such a flow could be provided by the highly exothermic catalytic reaction (G° of -209 kJ/mol).²⁴

Substrate flowing through catalase is conceptually analogous to solute flowing through membrane transport proteins, and the similarity is strengthened when the structures of catalases and some porins are compared. Both catalases and porins have a β barrel core surrounding a funnel shaped channel leading to a narrow hydrophobic constriction, which provides specificity to the substrate being transported.²⁵ The hydrophobic region of the porin channel has been implicated as a facilitator, or “grease slide,” for the flow of hydrophilic metabolites,²⁵ and the hydrophobic constriction of catalase may be ascribed a similar role in favoring H₂O₂ movement. The channel lengths are similar in both types of proteins with a porin spanning a 50-Å membrane compared with the approximately 60 Å combined length of the proposed inlet and exit channels in a catalase. Porins provide an efficient flow of specific substrates across the membrane, and catalases provide an efficient flow of H₂O₂ to the active site and of O₂ and H₂O to the outside. The importance of channel architecture leading to the active center is illustrated by the 2.5-fold increase in turnover rate in HP11 resulting from the single change of Arg260 to Ala located 20 Å from the heme in the minor or lateral channel, a possible candidate for the exhaust channel.²⁶

Broken Molecular Symmetry

The observation that molecular symmetry of the variant breaks during soaking with H₂O₂ is a most intriguing

Fig. 3. Stereo views of the heme distal side of the His128Asn variant when free (A) or complexed with hydrogen peroxide (B). The solvent organization in the structure of the free variant is closely related to the one found in His128Ala (Fig. 2B). Hydrogen peroxide molecules found in the complex are labeled H1, H2, and H3 (B). Water labeling is as described for Fig. 1. The averaged omit ($F_o - F_c$) electron-density maps are both presented at 2.3-Å resolution to facilitate the comparison. Differences in the solvent organization in the two structures are evident. The electron densities corresponding to the three putative H₂O₂ molecules present an elongated shape with volumes and electron-density values that cannot be explained by simple combinations of water molecules (see text). Each of the three putative H₂O₂ molecules (blue) is situated between positions that correspond to the positions of two water molecules in the uncomplexed variant. [Color figure can be viewed in the online issue, which is available at www.interscience.wiley.com.]

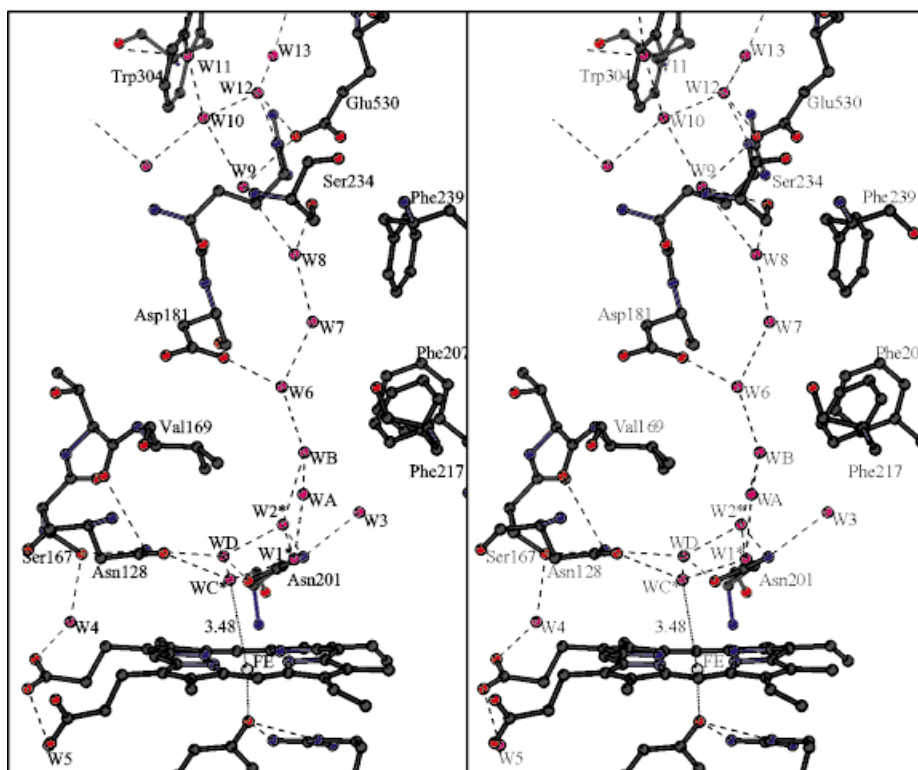
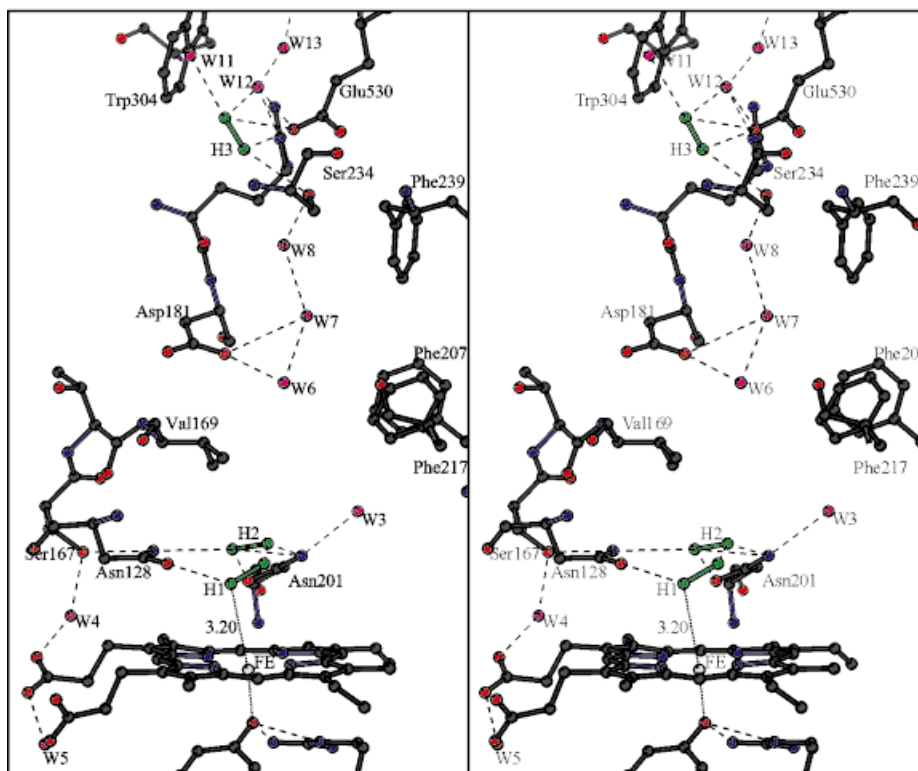
A - H128N**B - H128N-H₂O**

Figure 3.

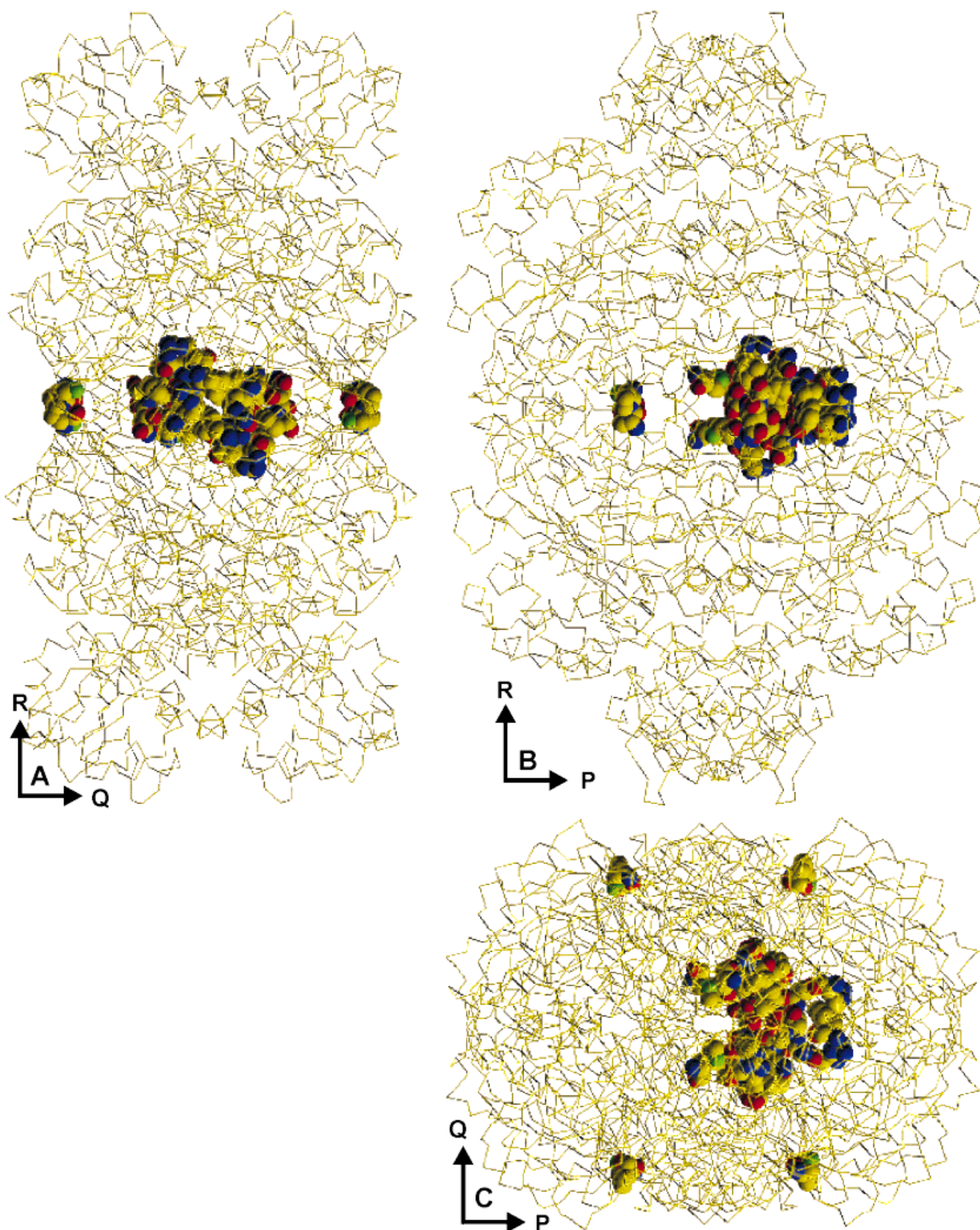


Fig. 4. Views down the molecular *P* (A), *Q* (B), and *R* (C) axes comparing the structures of the His128Asn variant free and complexed with H_2O_2 . Residues exhibiting the largest movement as a result of peroxide binding are displayed with a CPK representation. The heme residues are colored red. The subunits are color-coded: A, yellow; B, red; C, green; and D, cyan. Letters correspond to the PDB designations. The striking clustering of differences in subunits on one side of the cavity situated in the center of the molecular tetramer suggests an active role for the heme proximal side during catalysis. The departure from the original 222 molecular symmetry of the uncomplexed variant is also evident.

result that requires further investigation. Inter-subunit contacts between His449 residues along the molecular axis in native HP11,¹¹ already require small departures from perfect molecular symmetry and could be the trigger of an asymmetric behavior during catalysis. Deviations from perfect symmetry have also been reported for other catalases, particularly for HEC, where NADP(H) appears bound to only two of the subunits and where, in addition, compound I formation was shown to take place only in the two subunits lacking NADP(H). The apparent asymmetric structural features are consistent with classical kinetic studies that suggest only half of the heme groups are active simultaneously.²⁷ Hence, the departure from symmetry arising from peroxide binding is another indication that molecular symmetry can be easily broken during enzyme catalysis, which may allow for an unusual type of cooperativity among subunits. This, of course, leads to the underlying question as to how H₂O₂ binding and catalytic activity in two subunits interfere with or prevent activity in the other two subunits—a question that remains unanswered.

ACKNOWLEDGMENTS

Work in Barcelona was funded by grant BIO099-0865 from DGICYT (Spain) and by the European Union through the HCMP to Large Installations Project (contract CHGE-CT93-0040). Work in Winnipeg was supported by grant RGP9600 from the Natural Sciences and Engineering Research Council of Canada (NSERC). A NATO Collaborative Research Grant (SA-5-2-05) (to P.C.L. and I.F.) also supported the work. Fellowship SAP 1998-0087 from MEC (Spain) was awarded to W.M.A.

REFERENCES

- Murthy MRN, Reid TJ, Sicignano A, Tanaka N, Rossmann MG. Structure of beef liver catalase. *J Mol Biol* 1981;152:465–499.
- Fita I, Silva AM, Murthy MRN, Rossmann MG. The refined structure of beef liver catalase at 2.5 Å resolution. *Acta Crystallogr B* 1986;42:497–515.
- Putnam CD, Arval AS, Bourne Y, Tainer JA. Active and inhibited human catalase structures: ligand and NADPH binding and catalytic mechanism. *J Mol Biol* 2000;296:295–309.
- Ko TP, Safo MK, Musayev FN, Di Salvo ML, Wang C, Wu, SH, Abraham DJ. Structure of human erythrocyte catalase. *Acta Crystallogr D Biol Crystallogr* 2000;56:241–245.
- Vainshtein BK, Melik-Adamyany WR, Barynin VV, Vagin AA, Grebenko AI, Borisov VV, Bartels KS, Fita I, Rossmann MG. Three-dimensional structure of catalase from *Penicillium vitale* at 2.0-Å resolution. *J Mol Biol* 1986;188:49–61.
- Melik-Adamyany WR, Barynin VV, Vagin AA, Borisov VV, Vainshtein BK, Fita I, Murthy MRN, Rossmann MG. Comparison of beef liver and *Penicillium vitale* catalases. *J Mol Biol* 1986;188:63–72.
- Maté MJ, Zamocky M, Nykyri LM, Herzog C, Alzari PM, Betzel C, Koller F, Fita, I. Structure of catalase-A from *Saccharomyces cerevisiae*. *J Mol Biol* 1999;286:135–149.
- Gouet P, Jouve HM, Dideberg O. Crystal structure of *Proteus mirabilis* PR catalase with and without bound NADPH. *J Mol Biol* 1995;249:933–954.
- Murshudov GN, Melik-Adamyany WR, Grebenko AI, Barynin VV, Vagin AA, Vainshtein BK, Dauter Z, Wilson KS. Three-dimensional structure of catalase from *Micrococcus lysodeikticus* at 1.5 Å resolution. *FEBS Lett* 1992;312:127–131.
- Bravo J, Verdagner N, Tormo J, Betzel C, Switala J, Loewen PC, Fita I. Crystal structure of catalase HP11 from *Escherichia coli*. *Structure* 1995;3:491–502.
- Bravo J, Maté MJ, Schneider T, Switala J, Wilson K, Fita I, Loewen PC. Structure of catalase HP11 from *Escherichia coli* at 1.9Å resolution. *Proteins* 1999;34:155–166.
- Murshudov GN, Grebenko AI, Barynin V, Dauter Z, Wilson KS, Vainshtein BK, Melik-Adamyany W, Bravo J, Ferrán JM, Ferrer JC, Switala J, Loewen PC, Fita I. Structure of the heme d of *Penicillium vitale* and *Escherichia coli* catalases. *J Biol Chem* 1996;271:8863–8868.
- Bravo J, Fita I, Ferrer JC, Ens W, Hillar A, Switala J, Loewen PC. Identification of a novel bond between a histidine and the essential tyrosine in catalase HP11 of *Escherichia coli*. *Protein Sci* 1997;6:1016–1023.
- Loewen PC, Switala J, von Ossowski I, Hillar A, Christie A, Tattrie B, Nicholls P. Catalase HP11 of *Escherichia coli* catalyzes the conversion of protoheme to cis-heme d. *Biochemistry* 1993;32:10159–10164.
- Otwinowski Z, Minor W. Processing of X-ray diffraction data collected in oscillation mode. *Methods Enzymol* 1996;276:307–326.
- Brünger AT. XPLOR Manual. Version 3. New Haven, CT: Yale University; 1992.
- Murshudov GN, Vagin AA, Dodson EJ. Refinement of macromolecular structures by the maximum-likelihood method. *Acta Crystallogr D Biol Crystallogr* 1997;53:240–255.
- Perrakis A, Morris RJH, Lamzin VS. Automated protein model building combined with iterative structure refinement. *Nature Struct Biol* 1999;6:458–463.
- Jones TA, Zou JY, Cowan SW, Kjeldgaard M. Improved methods for building protein models in electron density maps. *Acta Crystallogr A* 1991;47:110–119.
- Kleywegt GJ, Jones TA. Detection, delineation, measurement and display of cavities in macromolecule structures. *Acta Crystallogr D Biol Crystallogr* 1994;50:178–185.
- Maté MJ, Sevinc MS, Hu B, Bujons J, Bravo J, Switala J, Ens W, Loewen PC, Fita I. Mutants that alter the covalent structure of catalase hydroperoxidase II from *Escherichia coli*. *J Biol Chem* 1999;274:27717–27725.
- Nicholls P, Fita I, Loewen PC. Enzymology and structure of catalases. *Adv Inorg Chem* 2001;51:51–106.
- Chu K, Vojtchovsky J, McMahon BH, Sweet RM, Berendzen J, Schlichting I. Structure of a ligand-binding intermediate in wild-type carbonmonoxy myoglobin. *Nature* 2000;403:921–923.
- Nicholls P, Schonbaum GR. Catalases. The enzymes. Vol 8. 2nd ed. New York: Academic Press; 1963. p 147–217.
- Forst D, Welte W, Wacker T, Diederichs K. Structure of the sucrose-specific porin SerY from *Salmonella typhimurium* and its complex with sucrose. *Nature Struct Biol* 1998;5:37–45.
- Sevinc MS, Maté MJ, Switala J, Fita I, Loewen PC. Role of the lateral channel in catalase HP11 of *Escherichia coli*. *Protein Sci* 1999;8:490–498.
- Chance B, Oshino N. Kinetics and mechanisms of catalase in peroxisomes of the mitochondrial fraction. *Biochem J* 1971;122:225–233.